Cardiovascular Research (2014) **103**, 217–227
doi:10.1093/cvr/cvu138

CXCR3-independent actions of the CXC chemokine CXCL10 in the infarcted myocardium and in isolated cardiac fibroblasts are mediated through proteoglycans

Amit Saxena[1], Marcin Bujak[2], Olga Frunza[1], Marcin Dobaczewski[1,2], Carlos Gonzalez-Quesada[1,2], Bao Lu[3], Craig Gerard[3], and Nikolaos G. Frangogiannis[1,2]*

[1]The Wilf Family Cardiovascular Research Institute, Department of Medicine (Cardiology), Albert Einstein College of Medicine, 1300 Morris Park Avenue Forchheimer G46B, Bronx, NY 10461, USA; [2]Department of Medicine, Baylor College of Medicine, Houston, TX, USA; and [3]Boston Children's Hospital, Harvard Medical School, Boston, MA, USA

Received 14 April 2014; accepted 25 May 2014; online publish-ahead-of-print 1 June 2014

Time for primary review: 40 days

Aims The CXC chemokine CXCL10 is up-regulated in the infarcted myocardium and limits cardiac fibrosis by inhibiting growth factor-mediated fibroblast migration. CXCL10 signals by binding to its receptor CXCR3; however, recently CXCR3-independent CXCL10 actions have been suggested. Our study explores the role of CXCR3 signalling in myocardial infarction and investigates its involvement in mediating the anti-fibrotic effects of CXCL10.

Methods and results Wild-type and CXCR3 null mice underwent reperfused infarction protocols. CXCL10 was markedly induced in the infarct; in contrast, expression of the other two CXCR3 ligands, CXCL9 and CXCL11 was extremely low. CXCR3 loss did not affect scar size, geometric ventricular remodelling, collagen deposition, and systolic dysfunction of the infarcted heart. CXCR3 null mice had increased peak neutrophil recruitment and delayed myofibroblast infiltration in the infarcted heart, but exhibited comparable myocardial expression of pro-inflammatory cytokines and chemokines. *In vitro*, CXCL10 did not modulate Transforming Growth Factor (TGF)-β signalling, but inhibited basic fibroblast growth factor (bFGF)-induced cardiac fibroblast migration in both wild-type and CXCR3 null cells. Treatment of fibroblasts with heparinase and chondroitinase to cleave glycosaminoglycan chains abrogated the inhibitory effects of CXCL10 on cell migration.

Conclusion CXCR3 signalling does not critically regulate cardiac remodelling and dysfunction following myocardial infarction. The anti-fibrotic effects of CXCL10 in the healing infarct and in isolated cardiac fibroblasts are CXCR3-independent and may be mediated through proteoglycan signalling. Thus, administration of CXCR3-defective forms of CXCL10 may be an effective anti-fibrotic strategy in the remodelling myocardium without activating a potentially injurious, CXCR3-driven T cell response.

Keywords Myocardial infarction • Fibroblast • Chemokine • Proteoglycan • Cardiac remodeling

1. Introduction

Chemokine induction is a hallmark of the inflammatory and reparative response following myocardial infarction.[1,2] Members of both major subfamilies of chemokines are released in the infarcted myocardium, bind to glycosaminoglycans on the endothelial surface and interact with the corresponding chemokine receptors expressed by leucocytes, playing an important role in chemotaxis of leucocyte subpopulations. CXC chemokines containing the ELR motif (such as interleukin-8 in higher mammals and the corresponding CXCR2 ligands in rodents) are rapidly up-regulated in the infarcted heart and mediate recruitment of neutrophils into the healing infarct.[3,4] Members of the CC chemokine subfamily on the other hand, attract mononuclear cell subsets, orchestrating the post-infarction inflammatory reaction. CCL2/Monocyte Chemoattractant Protein (MCP)-1 is a key mediator in the recruitment of pro-inflammatory and phagocytotic monocytes,[5,6] whereas CCR5

* Corresponding author. Tel: +1 718 430 3546; fax: +1 718 430 8989, Email: nikolaos.frangogiannis@einstein.yu.edu

ligands may attract subpopulations of inhibitory mononuclear cells suppressing the post-infarction inflammatory response.[7]

In addition to their established role in leucocyte trafficking, chemokines may also modulate behaviour, differentiation, and function of non-haematopoietic cells. The ELR-negative CXC chemokine CXCL10/Interferon-γ-inducible protein (IP)-10 modulates endothelial cell and fibroblast phenotype inducing potent angiostatic and anti-fibrotic effects. We have previously demonstrated that CXCL10 is markedly up-regulated in myocardial infarction[8] and protects the heart from excessive fibrotic remodelling by inhibiting growth factor-induced fibroblast migration.[9] CXCR3, the only well-characterized functional receptor for CXCL10,[10] is known to activate pro-inflammatory Th1 lymphocyte responses.[11] In addition to CXCL10, CXCR3 also binds two other interferon-γ-inducible CXC chemokines: CXCL9/Monokine induced by interferon-γ (Mig) and CXCL11/ITAC (Interferon-inducible T cell alpha chemoattractant). Both *in vitro* and *in vivo* studies have suggested that in addition to CXCR3, CXCL10 may also signal through other functional receptors;[12,13] however, the relative significance of CXCR3-independent CXCL10 signalling remains unknown.

Our current study examines the role of CXCR3 signalling in the infarcted heart. Our *in vivo* and *in vitro* studies suggest that the anti-fibrotic effects of CXCL10 on the remodelling infarcted heart are mediated through CXCR3-independent mechanisms and may involve proteoglycan signalling. Our findings may have important therapeutic implications, suggesting that CXCL10 defective in CXCR3 signalling[13] may attenuate fibrotic cardiac remodelling without exerting potentially injurious pro-inflammatory CXCR3-mediated effects.

2. Methods

2.1 Animal protocols

Animal studies were approved by the Institutional Animal Care and Use Committee at Baylor College of Medicine and at Albert Einstein College of Medicine and conform with the Guide for the Care and Use of Laboratory Animals published by the National Institutes of Health. Female and male C57/BL6 mice and CXCR3 KO mice in a C57BL6 background, 2–4 months of age, were anaesthetized using inhaled isoflurane (4% for induction, 2% for maintenance). WT and CXCR3 KO mice used for *in vivo* experiments were from our own colony.[14] For the *in vitro* studies, CXCR3 mice used to harvest cardiac fibroblasts were purchased from Jackson labs (B6.129P2-Cxcr3^{tm1Dgen}/J)[15] along with corresponding C57BL6J controls. For analgesia, buprenorphine (0.05–0.2 mg/kg s.c.) was administered at the time of surgery and q12 h thereafter for 2 days. Additional doses of analgesics were given if the animals appeared to be experiencing pain (based on criteria such as immobility and failure to eat). Intraoperatively, heart rate, respiratory rate, and electrocardiogram were continuously monitored and the depth of anaesthesia was assessed using the toe pinch method. A closed-chest model of reperfused myocardial infarction was utilized,[16] in order to avoid the confounding effects of surgical trauma and inflammation. The left anterior descending coronary artery was occluded for 1 h then reperfused for 6 h, 24 h, 3 days, 7 days, or 28 days. To assess cardiac function and remodelling following myocardial infarction, animals in the 7-day group underwent baseline and pre-sacrifice echocardiographic analysis (WT $n = 14$, KO $n = 12$). An additional group of WT and CXCR3 KO mice undergoing 28-day protocols ($n = 12$/group) had echocardiography only after 28 days of reperfusion. Additional groups of mice underwent quantitative morphometric analysis after 7 days (WT $n = 15$, KO $n = 13$) or 28 days (WT $n = 13$, KO $n = 6$) of reperfusion. At the end of the experiment, euthanasia was performed using 2% inhaled isoflurane followed by cervical dislocation. Early euthanasia was performed with the following criteria, indicating suffering of the animal: weight loss $>20\%$, vocalization, dehiscent wound, hypothermia, clinical signs of heart failure (cyanosis, dyspnoea, tachypnoea), lack of movement, hunched back, ruffled coat, lack of food or water ingestion. The heart was perfusion-fixed in zinc–formalin, and embedded in paraffin for histological studies. Additional mice underwent 6 or 24 h reperfusion protocols ($n = 9$/group) and the hearts were used for RNA extraction. To assess leucocyte and myofibroblast infiltration, hearts were immersion-fixed in zinc–formalin and embedded in paraffin for routine histological analysis (24 h reperfusion: WT $n = 10$, KO $n = 7$; 72 h reperfusion: WT $n = 12$ KO $= 7$; 7 days reperfusion WT $n = 12$ KO $= 9$). Sham animals (WT $n = 4$/group) were prepared identically without undergoing coronary occlusion/reperfusion.

2.2 Perfusion fixation and morphometric assessment of ventricular volumes

Perfusion-fixed hearts were used for morphometric assessment of post-infarction remodelling.[17] A cardioplegic solution was perfused through the jugular vein to promote relaxation. Hearts were fixed for 10 min with 10% zinc buffered formalin by aortic perfusion. The entire heart was cross-sectioned from base to apex at 250 μm intervals. Ten serial 5 μm sections were obtained at each interval, corresponding to an additional 50 μm segment. The first section from each interval was stained with haematoxylin/eosin. For each section, the left-ventricular wall area, septal area, left-ventricular chamber area, and the infarct area were measured using Image Pro software. Cardiac end-diastolic volumes and scar size were measured by calculating the sum of the volumes of all 300 μm partitions.

2.3 Echocardiography

Transthoracic echocardiography (short-axis views at the mid-papillary level) was performed using the Vevo 770 system (Visualsonics). LV end-diastolic diameter (LVEDD), fractional shortening (FS), and LV mass were measured as indicators of function and remodelling. The percent changes in these parameters at 7 days after infarction were calculated using the following formulas: $\Delta\text{LVEDD} = 100 \times (\text{LVEDD}_{7d} - \text{LVEDD}_{pre})/\text{LVEDD}_{pre}$, $\Delta\text{LVmass} = 100 \times (\text{LVmass}_{7d} - \text{LVmass}_{pre})/\text{LVmass}_{pre}$, and $\Delta\text{FS} = 100 \times (\text{FS}_{pre} - \text{FS}_{7d})/\text{FS}_{pre}$. Additional groups of WT and CXCR3 KO mice were imaged only after 28 days of reperfusion.

2.4 Immunohistochemistry

Histological sections were stained immunohistochemically with the following antibodies: anti-α-smooth muscle actin (α-SMA) antibody (Sigma, St Louis, MO, USA), rat anti-mouse macrophage antibody Mac-2 (Cedarlane), and rat anti-neutrophil antibody (Serotec, Raleigh, NC, USA). Staining was performed using a peroxidase-based technique as previously described.[5] Quantitative assessment of neutrophil and macrophage density was performed by counting the number of neutrophils and Mac-2-immunoreactive cells, respectively, in the infarcted area. Myofibroblasts were identified as spindle-shaped α-SMA+ cells located outside the vascular media and their density was measured in the infarcted area. Immunofluorescent staining was performed using a rabbit anti-CXCR3 antibody (Bioss Antibodies, Woburn, MA, USA) and a rat anti-heparan sulfate (HS) antibody (Abcam, Cambridge, MA, USA). For cellular localization studies, dual immunofluorescence combining CXCR3/α-SMA, CXCR3/Mac2, and heparan sulfate/α-SMA staining was performed. Collagen content in the infarcted heart, infarct border zone, and non-infarcted remote remodelling myocardium was assessed through quantitation of the collagen area in Sirius red-stained sections as previously described.[18]

2.5 RNA extraction, ribonuclear protection assay, and qPCR

Hearts were harvested after 6–24 h of reperfusion; infarcted and non-infarcted segments were separated by visual inspection. mRNA was extracted from each segment. mRNA expression level of the cytokines Interleukin (IL)-1β, IL-6, Transforming Growth Factor (TGF)-β1, 2, and 3, and the chemokines MCP-1 and MIP-2 was assessed using a ribonuclear protection

Table 1 qPCR primers

	Forward	Reverse
CXCL10/IP-10	TTCTTTAAGGGCTGGTCTGAG	GTCGCACCTCCACATAGC
CXCL9/Mig	CTGGAGCAGTGTGGAGTTC	CCGTTCTTCAGTGTAGCAATG
CXCL11/ITAC	GTTGAAGTGATTGTTACTATGAAG	TGGCACAGAGTTCTTATTGG
CXCR3	GCCTGAACTTTGACAGAA	GGAAGAGTTAACACCAGC

assay (RiboQuant; Pharmingen).[16] Gene expression was normalized to 18S L32 mRNA. Expression levels of CXCR3 and the CXCR3 ligands CXCL10/IP-10, CXCL11/I-TAC, and CXCL9/Mig were measured using qPCR.[19] The primer sequences are listed in *Table 1*.

2.6 Isolation of WT and CXCR3 null cardiac fibroblasts and transwell migration assay

Mouse cardiac fibroblasts were isolated from WT and CXCR3 KO hearts by enzymatic digestion with a collagenase buffer as previously described.[9,20] Fibroblast migration was studied using the colorimetric transwell system QCM™ (Millipore Corporation, Billerica, MA, USA). Fibroblasts used in the assay were serum starved for 24 h prior to the experiment. Cells were harvested using TrypLe express (GIBCO Invitrogen Corporation, Carlsbad, CA), counted and reconstituted with serum-free DMEM/F12 (GIBCO Invitrogen Corporation, Carlsbad, CA, USA) to bring the cells to concentration of 5×10^5 cells/mL. Cell suspensions were stimulated with vehicle or recombinant mouse CXCL10 (R&D systems, Mineapolis, MN, USA) (100 ng/mL) and incubated for 1 h. Subsequently, 300 μL of CXCL10-treated or control cell suspensions were added to the upper chamber. A total of 500 μL of serum-free DMEM/F12 or 20 ng/mL bFGF DMEM/F12 were added to the lower chamber and incubated for 4 h at 37°C in 5% CO_2. After incubation, remaining cell suspensions from upper wells were removed and inserts were placed in cell stain solution for 20 min at room temperature. Subsequently, inserts were collected and rinsed several times in distilled water. Migrated cells were visualized and photographed using an inverted microscope. Optical density of dye extract was measured at 560 nm using a NanoDrop spectrophotometer. Cell migration in each individual experiment was normalized to the level of migration in chamber without chemoattractant (control). In order to study the role of proteoglycan signalling in CXCL10-mediated modulation of cardiac fibroblast migration, WT cells were pre-treated with heparinase I or chondroitinase ABC (both from Sigma – final concentration 50 mU/mL) for 50 min and control cells, then used for migration assays. The effects of CXCL10 on bFGF-induced migration in the presence or absence of heparinase and chondroitinase were studied.

2.7 Western blotting

In order to study the effects of CXCL10 on the TGF-β/Smad cascade, isolated mouse cardiac fibroblasts were stimulated with CXCL10 (100 ng/mL) in the presence or absence of TGF-β1 (10 ng/mL) for 60 min or 4 h. At the end of the experiment, protein was extracted from the lysed cells. Western blotting for phosphorylated Smad2 (p-Smad2) and Smad2 was performed using antibodies from Cell Signaling. The ratio of p-Smad2:smad2 expression was measured.

2.8 Gel contraction assay

WT and CXCR3 KO cardiac fibroblasts were overnight serum starved. Collagen matrix was prepared by diluting a stock solution of rat 3.48 mg/mL collagen I (GIBCO Invitrogen Corporation, Carlsbad, CA, USA) with 2× DMEM and distilled water for a final concentration of 1 mg/mL collagen. CXCL10-stimulated and control cell suspensions were mixed with collagen solution to achieve the final 3×10^5 cells/mL concentration. Subsequently, 500 μL of this suspension was aliquoted to a 24-well culture plate (BD Falcon, San Jose, CA, USA) and allowed to polymerize at 37°C for 15 min. Following polymerization, pads were released from wells, transferred to six-well culture plate (BD Falcon, San Jose, CA, USA) and cultured in 0% FCS DMEM, 10% FCS DMEM, or 20 ng/mL bFGF DMEM, in the presence or absence of 100 ng/mL CXCL10. At 0 h and after 24 h, the pictures of the plates were taken in flatbed scanner and the area of each pad was measured using Image Pro software. In additional experiments, collagen pads populated with cardiac fibroblasts were used for RNA extraction as previously described,[21] or were processed for histological analysis.

2.9 Statistical analysis

Statistical analysis was performed using ANOVA followed by *t*-test corrected for multiple comparisons (Student–Newman–Keuls). Non-parametric ANOVA (Kruskall–Wallis) followed by Dunn's multiple comparison post-test was used when one or more data sets did not show Gaussian distribution. Data were expressed as mean ± SEM. Statistical significance was set at 0.05.

3. Results

3.1 Regulation of CXCR3 ligands in the infarcted myocardium

We used qPCR to study the regulation of CXCR3-activating chemokines in infarcted and non-infarcted myocardial segments from mice undergoing reperfused infarction protocols. In comparison to sham myocardium, CXCL10 mRNA expression was significantly up-regulated in the infarcted heart after 6–24 h of reperfusion ($P < 0.05$) (*Figure 1A*). CXCL11 mRNA levels in the infarcted myocardium were extremely low (10 000 times lower than corresponding CXCL10 levels); no statistically significant up-regulation of CXCL11 was noted in the infarct in comparison to the levels noted in sham hearts (*Figure 1B*). CXCL9 mRNA expression in the infarcted heart was also very low. There was a trend towards increased CXCL9 mRNA expression in the infarcted myocardium after 6 h of reperfusion (*Figure 1C*). Expression of all three CXCR3 ligands in non-infarcted segments from mice with reperfused infarction was not significantly different than in sham hearts (*Figure 1A–C*). We have previously demonstrated that CXCR3 mRNA levels are up-regulated in the infarcted myocardium.[16] In order to define the cellular identity of CXCR3+ cells in the infarcted myocardium, immunofluorescence was performed in reperfused mouse infarcts. After 72 h of reperfusion, CXCR3 immunoreactivity was localized in round and elongated cells infiltrating the infarct (*Figure 1D*). Dual immunofluorescence was used to examine whether CXCR3 is expressed by smooth muscle cells and infarct myofibroblasts. Vascular smooth muscle cells, identified as α-SMA-expressing cells located in the media did not express CXCR3; however, a subset of infarct myofibroblasts (identified

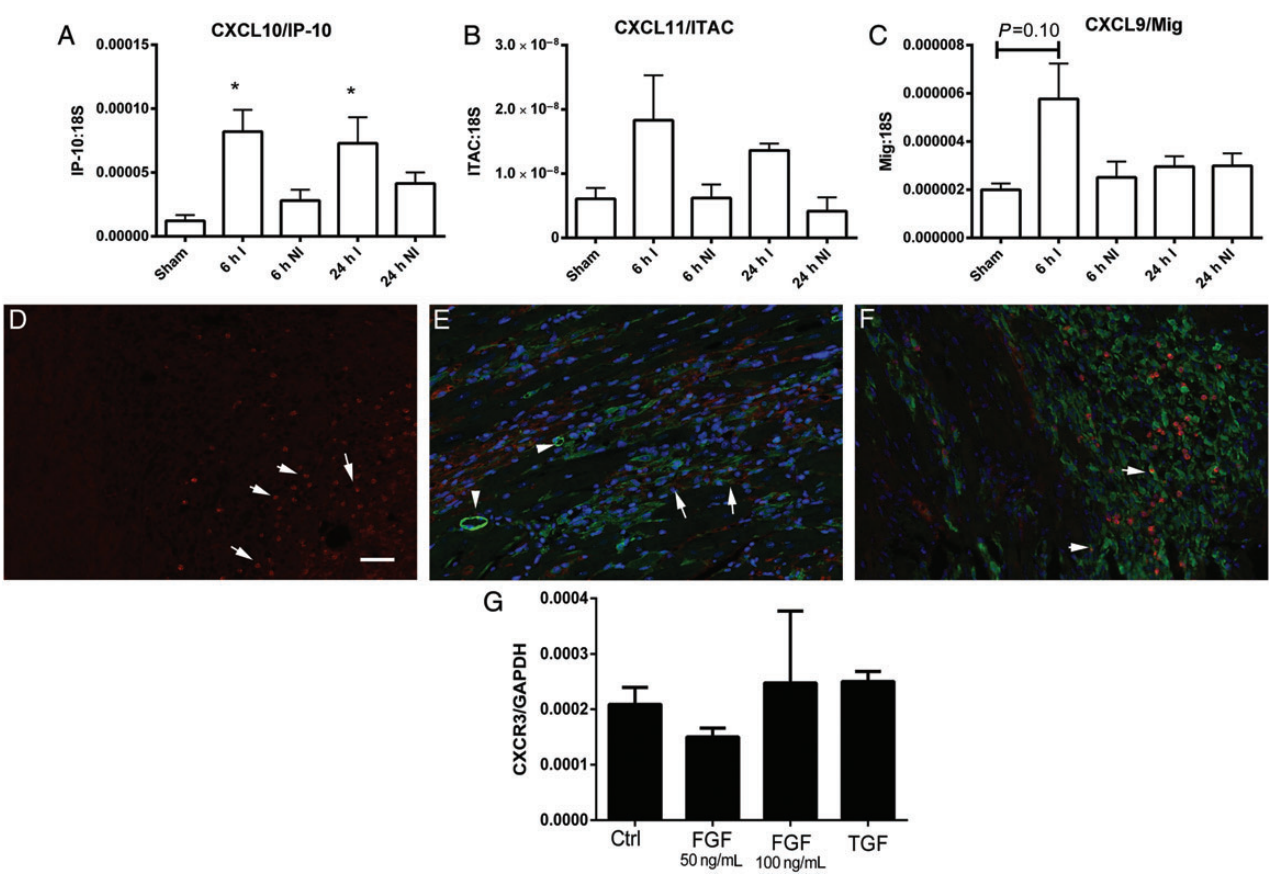

Figure 1 Regulation of CXCR3 ligand expression in reperfused mouse infarcts. (*A*) qPCR analysis showed marked up-regulation of CXCL10/IP-10 mRNA expression in infarcted segments (I) after 6–24 h of reperfusion, when compared with sham hearts. In contrast, non-infarcted (NI) segments had no significant increase in CXCL10 mRNA expression. (*B*) CXCL11/ITAC levels in sham and infarcted myocardium were extremely low (after normalization, CXCL11 mRNA levels in the infarcted myocardium were >5000 times lower than corresponding CXCL10 levels). There was no statistically significant difference in CXCL11 mRNA levels between infarcted and sham hearts. (*C*) CXCL9/Mig mRNA expression in the infarct was also low. A trend towards increased CXCL9 mRNA levels was noted after 6 h of reperfusion (*$P < 0.05$ vs. sham; infarction, $n = 6–9$/group, sham $n = 4$). (*D*) CXCR3 immunofluorescence identified abundant CXCR3+ cells in the infarcted myocardium after 72 h of reperfusion (arrows). (*E*) Dual immunofluorescence for CXCR3 (red) and α-SMA (green) showed that a subset of spindle shaped α-SMA+ myofibroblasts (arrows) expressed CXCR3. In contrast, smooth muscle cells, located in the vascular media (arrowheads) did not stain for CXCR3. Dual immunofluorescence for CXCR3 (red) and Mac2 (green) identified some of the CXCR3+ cells as macrophages (arrows). (*G*) *In vitro*, cardiac fibroblasts populating collagen pads expressed CXCR3 mRNA; stimulation with bFGF (50–100 ng/mL) or TGF-β1 (50 ng/mL) did not affect CXCR3 expression levels ($n = 4$). Scale bar = 50 μm.

as spindle-shaped interstitial α-SMA+ cells), exhibited CXCR3 immunoreactivity (*Figure 1E*). Dual staining for CXCR3 and Mac2 identified some CXCR3+ cells as macrophages (*Figure 1F*). *In vitro*, isolated cardiac fibroblasts populating collagen pads exhibited baseline expression of CXCR3 that was not significantly up-regulated upon stimulation with bFGF and TGF-β1 (*Figure 1G*).

3.2 CXCR3 absence does not affect post-infarction cardiac remodelling

We used two independent strategies, echocardiographic imaging and quantitative morphometric analysis, to examine the effects of CXCR3 loss on cardiac remodelling. Baseline function and chamber dimensions were comparable between WT and CXCR3 null mice, suggesting that CXCR3 absence does not affect cardiac homeostasis (*Table 2*). After 7 days of reperfusion, scar size was comparable between WT and CXCR3 null animals (*Figure 2A*). After 28 days of reperfusion, significant scar contraction was noted in both WT and KO animals; differences in scar size between WT and CXCR3 KO animals were not statistically significant. Morphometric analysis showed that WT and CXCR3 null animals had comparable dilative remodelling after 7 and 28 days of reperfusion (*Figure 2B*). Moreover, echocardiographic analysis demonstrated that after 7 days of reperfusion WT and CXCR3 null mice had comparable changes in systolic function, chamber dimensions, and left-ventricular mass (*Figure 2C–E*, *Table 2*). In mice undergoing 28-day reperfusion protocols, chamber dimensions, fractional shortening, and LV mass were comparable between WT and CXCR3 null animals (*Table 2*).

3.3 Effects of CXCR3 gene disruption on the post-infarction inflammatory response

Because CXCR3 signalling regulates inflammatory pathways, we examined whether CXCR3 loss affects the post-infarction inflammatory reaction. Following myocardial infarction, CXCR3 null mice had increased peak neutrophil infiltration after 24 h of reperfusion, but exhibited

Table 2 Echocardiographic assessment of cardiac function

	Pre		7 days		28 days	
	WT ($n = 14$)	KO ($n = 12$)	WT ($n = 14$)	KO ($n = 12$)	WT ($n = 12$)	KO ($n = 12$)
LVEDD (mm)	3.37 ± 0.06	3.29 ± 0.05	3.74 ± 0.07[a]	3.54 ± 0.06[b]	4.15 ± 0.13	4.03 ± 0.21
FS, %	42 ± 1	40 ± 2	35 ± 1[a]	31 ± 2[a]	27 ± 3	21 ± 7
LV mass (mg)	126.1 ± 4.9	110.8 ± 5.1	140.9 ± 8.5	131.5 ± 5.3	135.4 ± 10.1	134.4 ± 12.1

LVEDD, left-ventricular end-diastolic diameter; FS, fractional shortening; LV mass, left-ventricular mass ([a]$P < 0.01$; [b]$P < 0.05$ vs. corresponding pre).

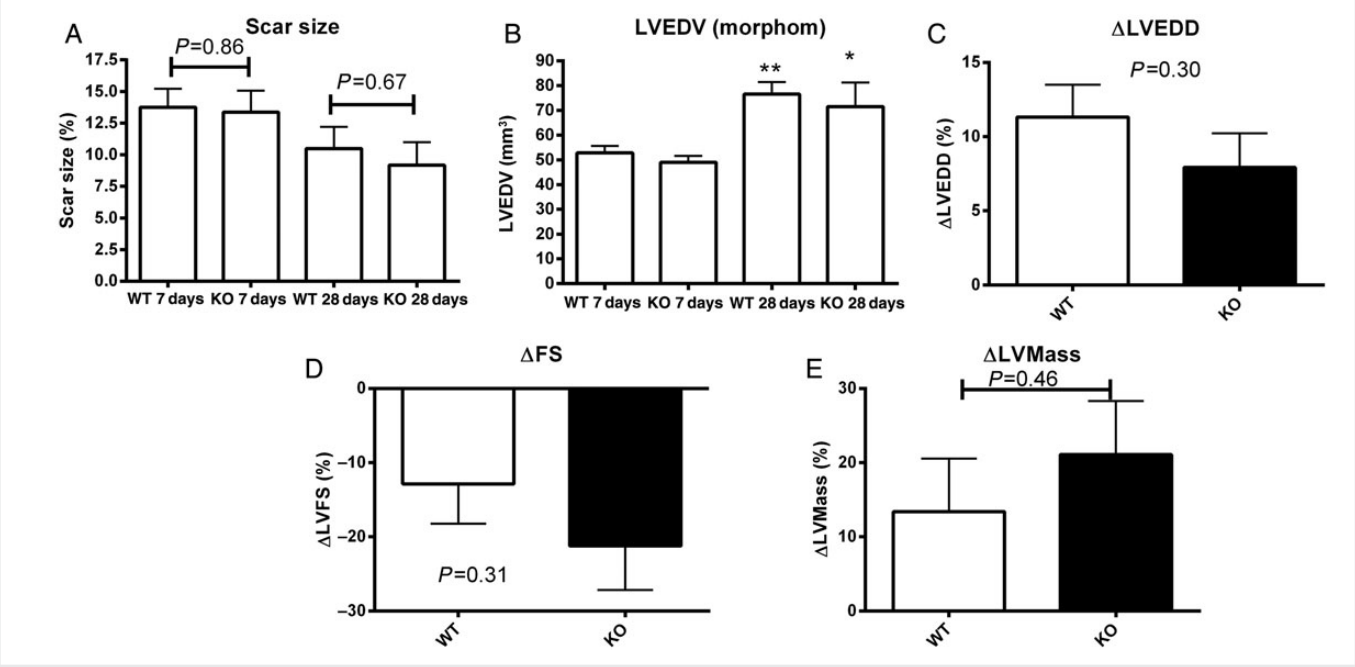

Figure 2 CXCR3 KO and WT animals have comparable scar size and post-infarction remodelling following ischaemia/reperfusion. (*A*) Quantitative morphometry was performed to measure the scar volume as a percentage of the total left-ventricular volume (scar size). After 7–28 days of reperfusion, scar size was comparable between WT and CXCR3 KO animals (7 days: WT $n = 15$, KO $= 13$; 28 days: WT $n = 13$, KO $n = 6$). (*B*) Quantitative morphometric analysis demonstrated that, when compared with WT animals, CXCR3 KO mice had comparable LVEDV after 7 and 28 days of reperfusion (*$P < 0.05$, **$P < 0.01$ vs. corresponding volume at 7 days). (*C–E*) Serial echocardiographic analysis showed that CXCR3 KO and WT mice had comparable changes in LVEDD, (*C*: ΔLVEDD), fractional shortening (*D*: ΔFS), and LV mass (*E*: ΔLV mass) following reperfused infarction (1 h occlusion/7 days reperfusion) (WT $n = 14$, KO $n = 12$).

timely clearance of the neutrophilic infiltrate (*Figure 3A–C*). Macrophage infiltration was also increased in CXCR3 null animals by about 20% after 7 days of reperfusion (*Figure 3D–F*). In comparison to non-infarcted areas of the myocardium, infarcted myocardial segments had significantly increased expression of the pro-inflammatory cytokines IL-1β and IL-6 (*Figure 4A* and *B*) and of the chemokines MCP-1 and MIP-2 (*Figure 4C* and *D*) in both WT and CXCR3 null animals. CXCR3 absence did not affect cytokine and chemokine synthesis in the infarcted myocardium (*Figure 4A–D*). In order to examine whether CXCR3 loss affects expression of its ligands in the infarcted heart, we compared expression of CXCL10, CXCL11, and CXCL9 in infarcted hearts (*Figure 4E–G*) after 6 and 24 h of reperfusion. At both timepoints, CXCL10 and CXCL11 levels were not affected by CXCR3 loss; however, CXCR3 knockouts exhibited a prolonged induction of CXCL9/Mig (*Figure 4G*).

3.4 CXCR3 loss delays infiltration of the infarcted myocardium with myofibroblasts

In reperfused murine myocardial infarction, WT mice exhibit rapid infiltration of the infarct border zone with α-SMA+ myofibroblasts after 72 h of reperfusion (*Figure 5A* and *B*). In comparison to WT animals, CXCR3 null mice had a delayed peak in infarct myofibroblast density (*Figure 5A–C*). Delayed myofibroblast infiltration in CXCR3 KO infarcts did not affect scar formation and fibrotic remodelling of the heart. Quantitative analysis of Sirius red-stained sections demonstrated that WT and CXCR3 KO hearts had comparable collagen content in the infarcted area, infarct border zone, and remote remodelling myocardium after 28 days of reperfusion (*Figure 5D–F*). mRNA expression of TGF-β isoforms in infarcted myocardial segments was also not affected by CXCR3 loss (*Figure 5G–I*).

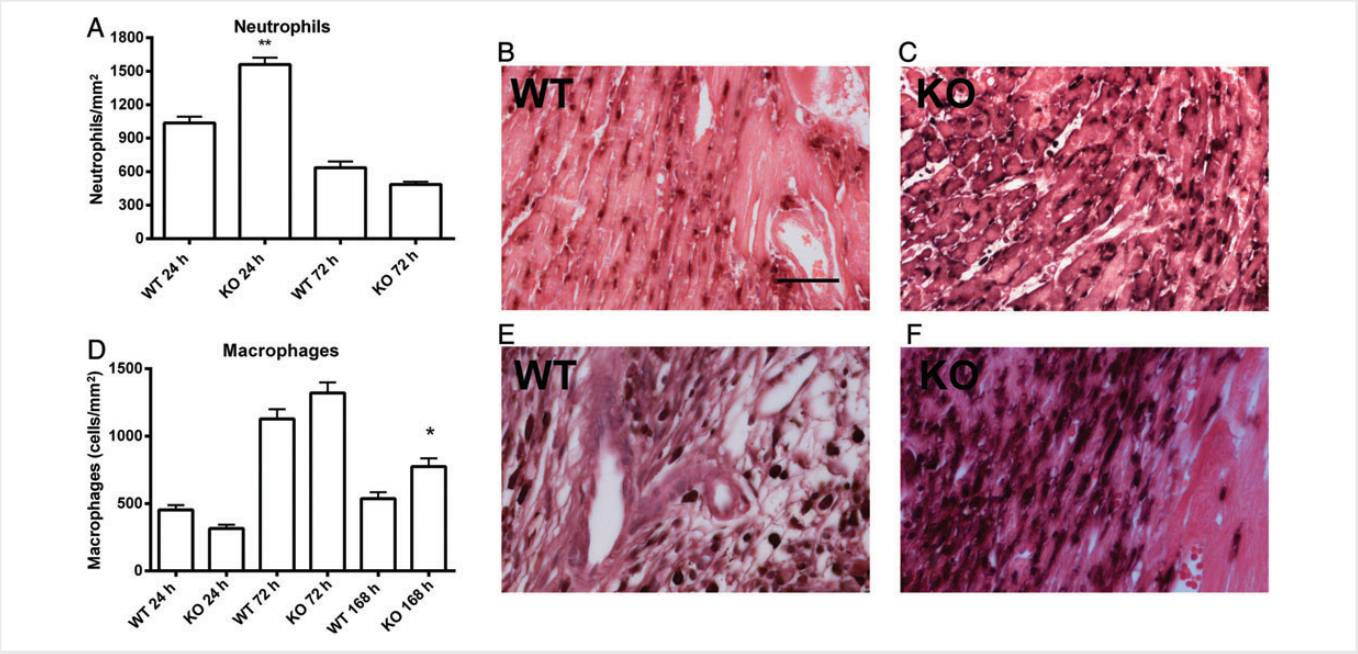

Figure 3 Effects of CXCR3 loss on infiltration of the infarcted myocardium with inflammatory leucocytes. (*A*) CXCR3 loss was associated with accentuated peak neutrophil infiltration after 24 h of reperfusion; however, after 72 h of reperfusion neutrophil density was comparable between groups. (*B* and *C*) Representative images show immunohistochemical staining for neutrophils (black) in WT (*B*) and CXCR3 KO (*C*) infarcts after 24 h of reperfusion. Peroxidase-bases staining was performed and developed with diaminobenzidine+nickel. Sections were counterstained with eosin. (*D*) Infarct macrophage density was comparable between WT and CXCR3 null animals after 24 −72 h of reperfusion. However, after 7 days of reperfusion, macrophage density was higher in CXCR3 KO infarcts. (*E* and *F*) Representative images show immunohistochemical staining for Mac2 (black) to identify macrophages in WT (*E*) and CXCR3 KO (*F*) infarcts after 7 days of reperfusion (**$P < 0.01$, *$P < 0.05$ vs. corresponding WT; 24 h: WT $n = 10$, KO $n = 7$; 72 h: WT $n = 12$, KO $n = 7$; 7 days: WT $n = 12$, KO $= 9$). Counterstained with eosin and haematoxylin. Scale bar = 40 μm.

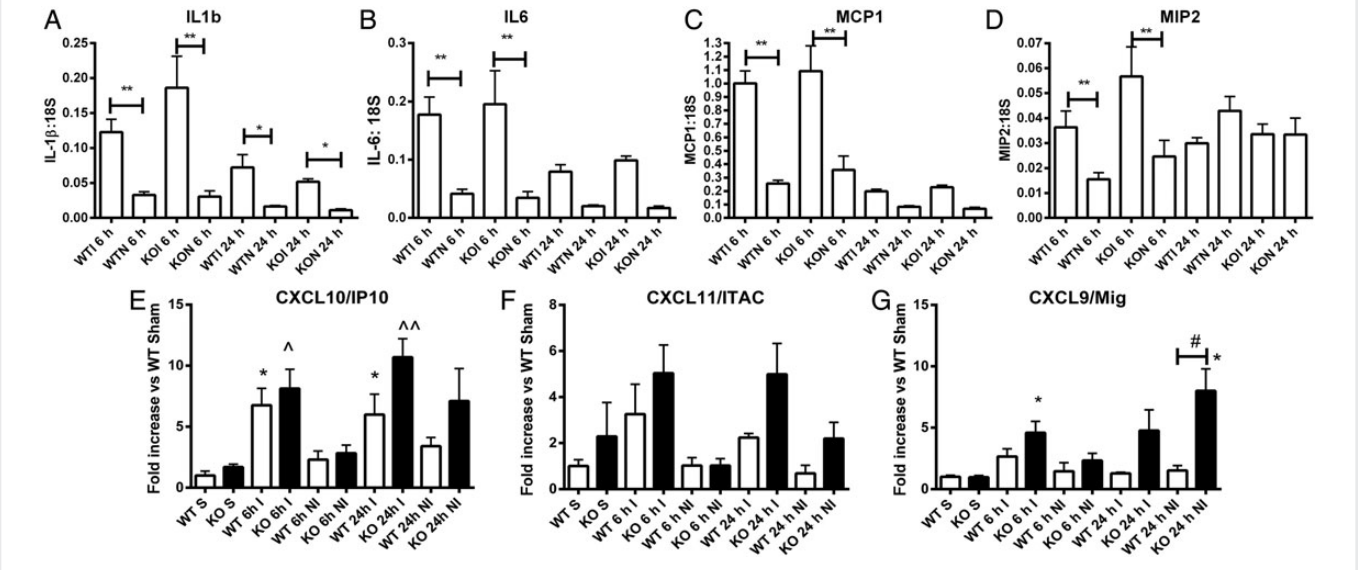

Figure 4 WT and CXCR3 KO mice have comparable myocardial cytokine and chemokine mRNA levels following myocardial infarction. (*A*–*D*) When compared with corresponding non-infarcted segments (N), infarcted myocardial segments harvested after 6 h of reperfusion (I) had significantly higher myocardial IL-1β (*A*), IL-6 (*B*), CCL2/MCP-1 (*C*), and CXCL2/MIP-2 (*D*) mRNA expression. However, no significant differences in cardiac cytokine and chemokine mRNA expression were noted between infarcted WT and CXCR3 KO animals (**$P < 0.01$ vs. corresponding non-infarcted segments, $n = 9$/group). *E*–*G*: Expression of the CXCR3 ligands CXCL10/IP-10 (*E*) and CXCL11/ITAC (*F*) was comparable between WT and KO mice after 6–24 h of reperfusion. When compared with WT animals, CXCR3 KO mice had prolonged myocardial up-regulation of CXCL9/Mig (*G*). *$P < 0.05$ vs. WT sham; ^$P < 0.05$, ^^$P < 0.01$ vs. KO sham.

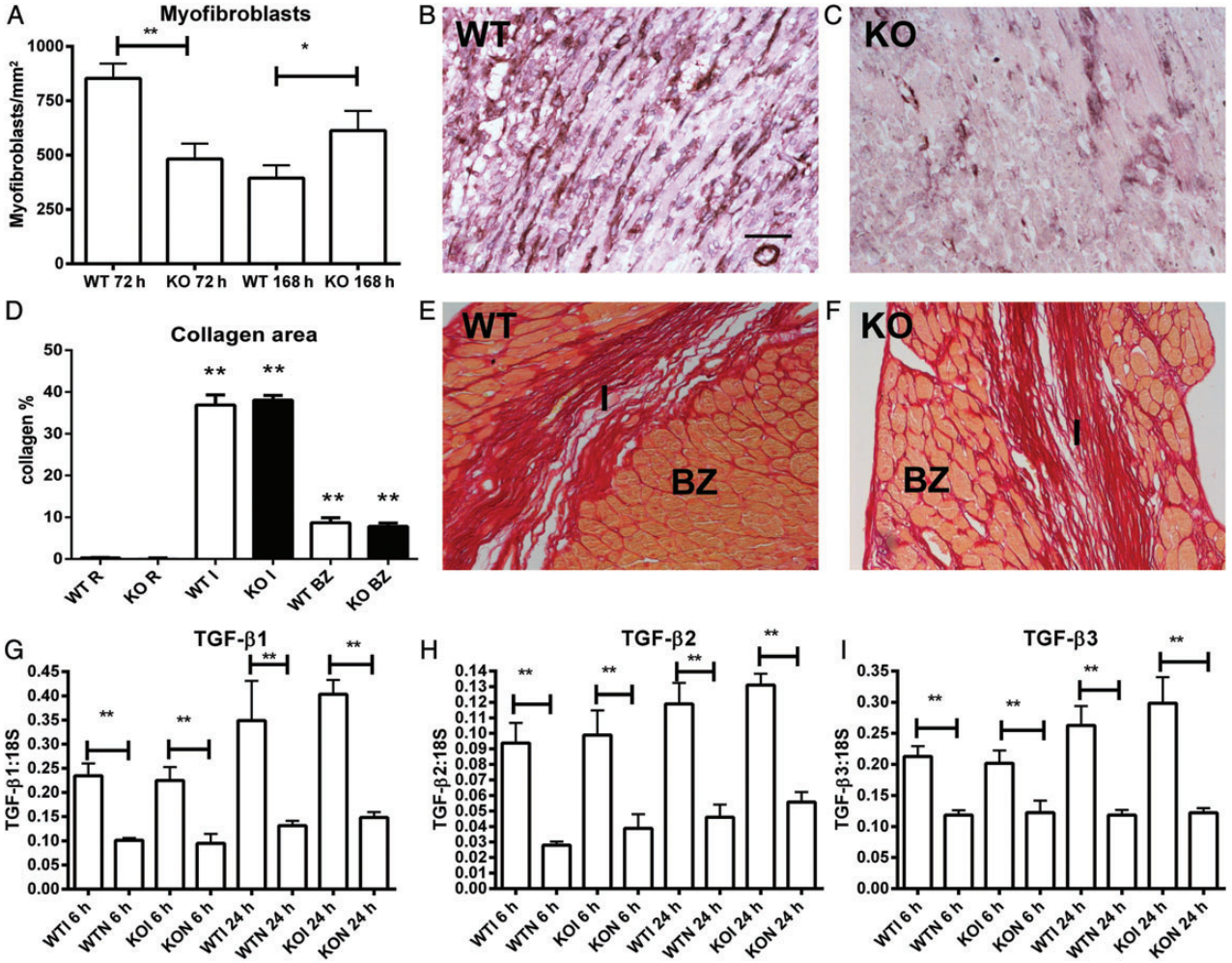

Figure 5 CXCR3 KO mice exhibit delayed infiltration of the infarct with myocfibroblasts. (*A*) The time course of myofibroblast infiltration in CXCR3 KO infarcts was delayed when compared with WT animals ($n = 7–12$/group). (*B* and *C*) Myofibroblasts in infarcted WT (*B*) and KO (*C*) hearts were identified through α-SMA immunohistochemistry (black) as spindle-shaped cells located outside the vascular media (counterstained with eosin). (*D–F*) Fibrotic remodelling of the infarcted heart was assessed by quantitation of collagen content in Sirius red-stained sections. WT and CXCR3 KO animals had comparable collagen content in the infarct (I), border zone (BZ), and remote remodelling myocardium (R) (**$P < 0.01$ vs. corresponding R; WT $n = 9$, KO $n = 6$). Representative images of reperfused infarcts after 28 days of reperfusion show collagen deposition in the infarct (I) and in the border zone (BZ) in WT (*E*) and KO animals (*F*). (*G–I*) In both WT and CXCR3 KO mice, myocardial TGF-β1, -β2, and -β3 mRNA expression was significantly higher in infarcted myocardial segments when compared with non-infarcted segments from the same heart (**$P < 0.01$ vs. corresponding non-infarcted segments, $n = 9$/group). However, WT and CXCR3 KO infarcts had comparable myocardial TGF-β isoform levels. Scale bar = 40 μm.

3.5 The inhibitory effects of CXCL10 on cardiac fibroblast migration are CXCR3-independent

We have previously demonstrated that CXCL10 loss results in increased fibrosis and accentuated adverse remodelling of the infarcted heart and demonstrated that CXCL10 inhibits growth factor-mediated cardiac fibroblast migration.[9] Because, in contrast to CXCL10 loss, deletion of its only known receptor, CXCR3, does not affect post-infarction cardiac remodelling, we examined whether CXCL10 exerts CXCR3-independent actions on isolated cardiac fibroblasts. In a transwell fibroblast migration assay, CXCL10 attenuated bFGF-induced fibroblast migration in WT cells (*Figure 6A*). CXCR3 null cardiac fibroblasts had decreased baseline fibroblast migration and a blunted migratory response to bFGF. However, much like in WT cells, CXCL10 decreased fibroblast migration in CXCR3 null cells suggesting that CXCL10-mediated inhibition of fibroblast migration is CXCR3-independent (*Figure 6A*).

3.6 The effects of CXCL10 on contraction of fibroblast-populated collagen gels are independent of CXCR3

Myofibroblast transdifferentiation is a key process in the reparative response following myocardial infarction; accumulation of fibroblasts expressing high levels of contractile proteins may play an important role in scar contraction and in the regulation of cardiac remodelling. We have previously demonstrated that CXCL10 augments growth factor-induced contraction of fibroblast-populated collagen pads; CXCL10 absence is associated with reduced scar contraction *in vivo*.

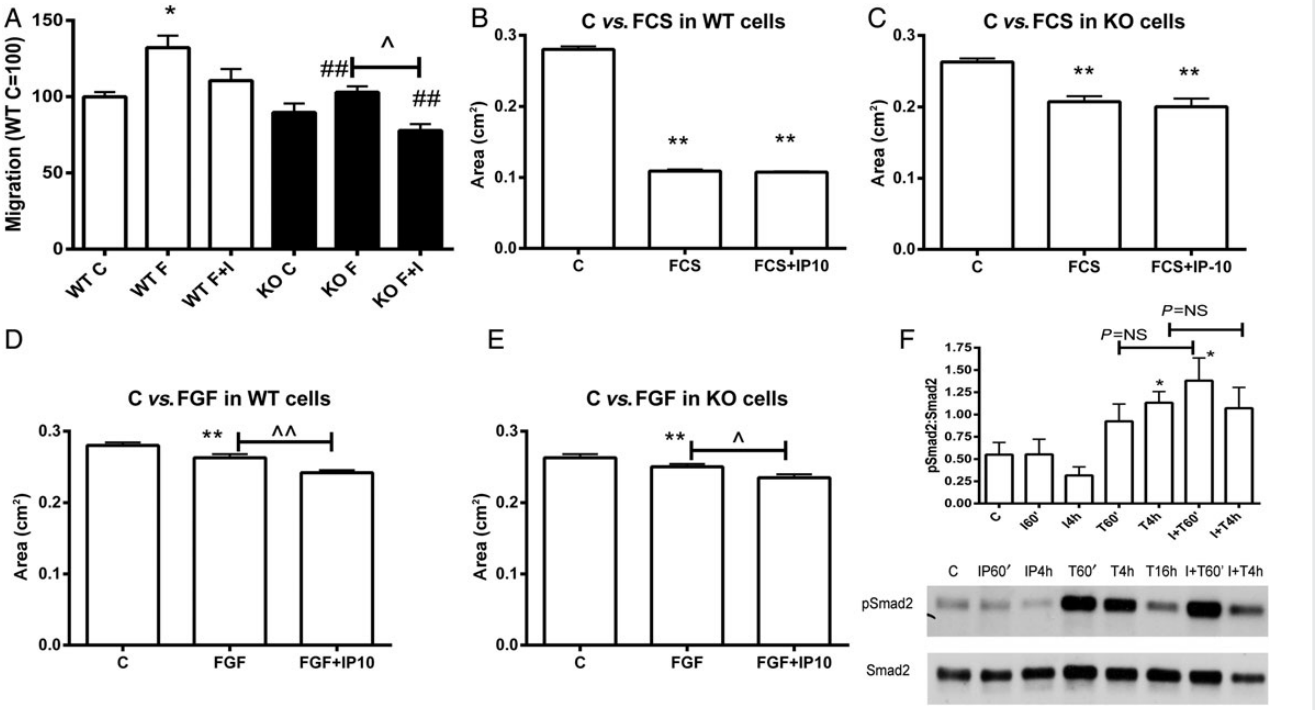

Figure 6 CXCL10/IP-10 inhibits growth factor-mediated cardiac fibroblast migration and enhances contraction of fibroblast-populated collagen pads in a CXCR3-independent manner. (*A*) A transwell migration assay was used to study the effects of CXCL10 on cardiac fibroblast migration. In WT cells, stimulation with bFGF induced fibroblast migration ($^{*}P < 0.05$); co-stimulation with CXCL10/IP-10 (I) attenuated the pro-migratory effects of bFGF (F). CXCR3 KO cells exhibited significantly attenuated migratory capacity in response to bFGF ($^{\#\#}P < 0.01$ vs. corresponding WT cells). However, CXCL10 attenuated FGF-induced fibroblast migration in CXCR3 KO cells ($^{\wedge}P < 0.05$), suggesting that the only well-characterized CXCL10 receptor is not required for the anti-migratory effects of the chemokine ($n = 3$). (*B*–*E*) Effects of CXCL10/IP-10 on contraction of fibroblast-populated collagen pads. (*B*) In collagen pads populated with WT cells, FCS stimulation caused marked contraction. CXCL10 stimulation did not affect FCS-induced collagen contraction. (*C*) Collagen pads populated with CXCR3 KO fibroblasts exhibited attenuated contraction when stimulated with FCS ($^{**}P < 0.01$ vs. control, $n = 8$). (*D* and *E*) bFGF stimulation induced contraction in collagen pads populated with WT (*D*) or CXCR3 KO (*E*) cells ($^{**}P < 0.01$ vs. control). Co-stimulation with CXCL10 enhanced bFGF-induced collagen contraction in pads populated with WT or CXCR3 KO cells ($^{\wedge}P < 0.05$, $^{\wedge\wedge}P < 0.01$ vs. FGF-stimulated, $n = 8$) suggesting that the effects of CXCL10 on cardiac fibroblast contractile activity are independent of CXCR3. (*F*) CXCL10 stimulation did not modulate TGF-β/Smad signalling in isolated cardiac fibroblasts. TGF-β1 stimulation (10 ng/mL) increased the expression of phosphorylated Smad2 (p-Smad2) by cardiac fibroblasts. CXCL10/IP-10 (I) stimulation (100 ng/mL) did not affect p-Smad2 levels in the presence or absence of TGF-β1 (T) ($^{*}P < 0.05$ vs. control, $n = 4$).

In order to test the hypothesis that the disparate effects of CXCL10 and CXCR3 loss in scar contraction may be due to CXCR3-independent actions of CXCL10, we compared contraction of collagen pads populated with WT and CXCR3 null cardiac fibroblasts. Stimulation with serum induced marked contraction of collagen pads populated with WT cardiac fibroblasts; the effects of serum were attenuated in CXCR3 null cells (*Figure 6B* and *C*). Upon serum stimulation, CXCL10 had no significant effects on gel contraction in both WT and CXCR3 null fibroblasts. bFGF stimulation also induced gel contraction in both WT and CXCR3 null fibroblasts (*Figure 6D* and *E*). CXCL10 augmented the effects of bFGF in both WT and CXCR3 null cells (*Figure 6D* and *E*), suggesting that the effects of CXCL10 on fibroblast contractile activity are CXCR3-independent.

3.7 CXCL10 does not modulate TGF-β-stimulated Smad signalling

In order to dissect the mechanisms of CXCL10-mediated anti-fibrotic actions, we examined whether CXCL10 modulates the TGF-β/Smad cascade, a key pathway in cardiac fibrosis. In isolated cardiac fibroblasts, TGF-β1 enhanced Smad2 phosphorylation; however CXCL10 stimulation had no effect on Smad activation in the presence or absence of TGF-β (*Figure 6F*).

3.8 The effects of CXCL10 on cardiac fibroblast migration are dependent on proteoglycan signalling

In order to examine whether the effects of CXCL10 on cardiac fibroblasts are mediated through proteoglycan signalling, we examined the effects of CXCL10 on growth factor-mediated migration of cells pre-treated with heparinase and chondroitinase. In a transwell assay bFGF induced fibroblast migration; CXCL10 stimulation attenuated cell migration. Pre-treatment with heparinase abrogated the effects of CXCL10 on bFGF-induced cardiac fibroblast migration. Pre-treatment with chondroitinase reduced bFGF-mediated migration, but also attenuated the inhibitory effects of CXCL10 on cell migration (*Figure 7A*). In order to examine the localization of proteoglycans in the infarcted myocardium, we performed immunofluorescent staining for HS. In normal

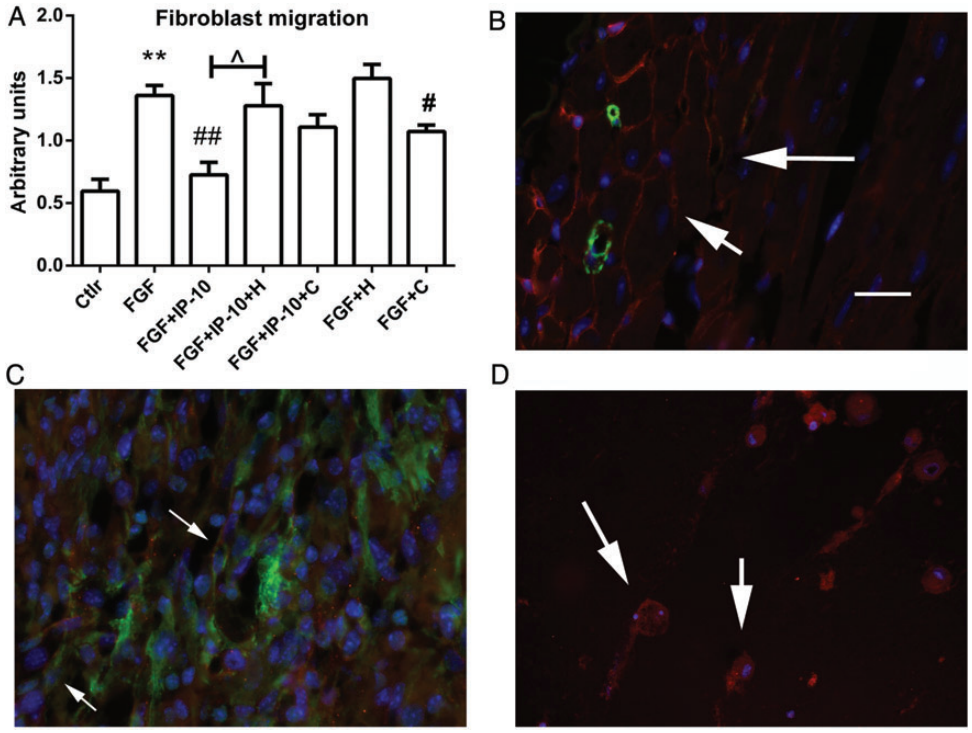

Figure 7 The inhibitory effects of CXCL10/IP-10 on fibroblast migration are mediated through proteoglycan signalling. (*A*) In a transwell assay, basic FGF induced fibroblast migration and CXCL10 inhibited FGF-mediated migration. Pre-treatment of fibroblasts with heparinase (*H*) abrogated the inhibitory effects of CXCL10. Pre-treatment with chondroitinase (*C*) attenuated FGF-induced migration, but also abrogated the inhibitory action of CXCL10 ($^{**}P < 0.05$ vs. C; $^{\#}P < 0.05$, $^{\#\#}P < 0.01$ vs. FGF, $n = 6$). (*B*) Dual immunofluorescence for α-SMA (green) and HS (red) localized HS in normal (*B*) and infarcted (*C*) myocardium. In normal hearts, HS staining labelled the interstitial matrix (*B*: arrows). After 72 h of reperfusion, HS was localized in the matrix and on spindle-shaped α-SMA+ myofibroblasts (*C*: arrows). (*D*) *In vitro* experiments showed that fibroblasts populating collagen pads expressed HS (arrows). Scale bar = 25 μm.

mouse hearts, HS localized in the interstitial matrix (*Figure 7B*). Dual immunofluorescence for HS and α-SMA demonstrated that in the infarcted myocardium HS localized in the matrix and in infarct myofibroblasts (*Figure 7C*). *In vitro*, cardiac fibroblasts populating collagen pads exhibited high expression of HS (*Figure 7D*).

4. Discussion

We have previously demonstrated that expression of the CXC chemokine CXCL10 and its receptor CXCR3 are markedly induced in canine and murine myocardial infarction.[8,16] Using CXCL10 null mice, we demonstrated that CXCL10 loss is associated with accentuated fibrosis and increased adverse remodelling of the infarcted heart.[9] CXCL10 exerts its anti-fibrotic actions, at least in part, through inhibition of fibroblast migration. Although CXCR3 is the only well-characterized receptor for CXCL10, a growing body of evidence suggests that certain effects of CXCL10 may be mediated through CXCR3-independent mechanisms. Our current investigation suggests that anti-fibrotic effects of CXCL10 on the infarcted heart are independent of CXCR3 and may involve proteoglycan signalling. CXCR3 absence did not affect geometric remodelling of the infarcted ventricle and did not affect scar formation in the infarcted heart. *In vitro*, CXCL10 inhibited growth factor-mediated fibroblast migration and enhanced contraction of fibroblast-populated pads in the presence or absence of CXCR3. Enzymatic depletion of HS and chondroitin sulfate (CS) chains abrogated the inhibitory effects of CXCL10 on fibroblast migration.

4.1 CXCR3 ligands in myocardial infarction

In addition to CXCL10, two other IFN-inducible, ELR-negative CXC chemokines, CXCL9/Mig and CXCL11/ITAC also signal through CXCR3. All three CXCR3 ligands are up-regulated in healing cutaneous wounds[22,23] in various types of inflammatory and allergic skin disorders[24,25] in experimental models of inflammatory nephritis[26] and in acute cardiac allograft rejection.[14] Our studies in reperfused mouse infarcts demonstrated that, of the three CXCR3 ligands studied, only CXCL10 expression shows robust and significant up-regulation in the infarcted myocardium. In contrast, CXCL9 and CXCL11 expression levels are very low in both sham and infarcted hearts (*Figure 1*). The distinct mechanisms involved in the regulation of CXCR3 ligands (due to the different regulatory elements in their promoters)[27] may explain their different patterns of expression in various types of tissue injury. Although CXCL10 synthesis is up-regulated by a wide range of pro-inflammatory mediators, including TLR ligands, IL-1β, and TNF-[8,28] (all rapidly released in the infarcted myocardium,[29,30] expression of CXCL9 and CXCL11 is more restricted and generally requires IFN-γ stimulation.[27,28] Thus, in the infarct environment, the predominance of IL-1/TLR and TNF-dependent signalling may selectively up-regulate CXCL10.

4.2 Effects of CXCR3 loss on the reparative fibrotic response following myocardial infarction

Because the adult mammalian heart has negligible regenerative capacity, repair of the infarcted myocardium is dependent on fibroblast activation and on formation of a collagen-based scar. Recruitment and activation of reparative cells in the healing infarct is dependent on timely induction and suppression of an inflammatory reaction; prolonged or overactive inflammation triggers protease activation causing dilative remodelling of the infarcted heart. Both morphometric and echocardiographic analysis showed that CXCR3 loss did not affect cardiac remodelling following infarction (*Figure 2*). After 7–28 days of reperfusion, scar size, chamber dimensions ,and systolic dysfunction were comparable between CXCR3 KO and WT animals (*Table 2*, *Figure 2*). Although loss of CXCR3 signalling did not affect the reparative and remodelling responses following infarction, CXCR3 null mice exhibited significant alterations in the cellular composition of the infarct. In the absence of CXCR3, early infiltration of the infarct with neutrophils was accentuated after 24 h of reperfusion and macrophage density was significantly increased after 72 h of reperfusion. However, these alterations in cellular composition of the infarct were not associated with significant changes in the expression of pro-inflammatory cytokines and chemokines (*Figure 4*), suggesting that CXCR3 does not have significant and consistent effects on the intensity of the post-infarction inflammatory response.

CXCR3 absence was associated with delayed infiltration of the infarcted myocardium with myofibroblasts, but did not affect fibrotic remodelling of the ventricle after 28 days of reperfusion (*Figure 5*). *In vitro* experiments suggested that delayed recruitment of fibroblasts in the absence of CXCR3 may reflect the attenuated migratory capacity of CXCR3 null cardiac fibroblasts in response to growth factors (*Figure 6A*). Experiments using human synovial fibroblasts isolated from patients with rheumatoid arthritis, suggested that CXCR3 blockade may reduce cellular invasiveness, interfering with reorganization of the actin cytoskeleton and inhibiting the formation of lamellipodia.[31]

The effects of CXCR3 in tissue inflammation, repair, and fibrosis appear to be dependent on the characteristics of the affected organ. Loss of CXCR3 signalling in models of cutaneous wounding resulted in delayed healing[32] and late development of a hypercellular and hypertrophic response,[33] associated with cellular proliferation. On the other hand, in a model of pulmonary fibrosis due to bleomycin-induced injury, CXCR3 loss increased mortality and accentuated fibroproliferation.[34] The organ-specific effects of CXCR3 signalling may reflect differential regulation of the three CXCR3 ligands in various models of injury. CXCL9 and CXCL11 are markedly up-regulated (along with CXCL10) in injured and fibrotic skin and lung.[35] In a model of hepatic fibrosis, endogenous CXCL9 exerted anti-fibrotic actions;[36] moreover, in pulmonary fibrosis, CXCL11 has been reported to exert anti-fibrotic actions presumed due to the attenuation of aberrant vascular remodelling.[37] In contrast, in the infarcted myocardium, where CXCL9 and CXCL11 are not significantly up-regulated, CXCL10 is the dominant CXCR3 ligand and appears to exert its effects, at least in part through CXCR3-independent actions.

4.3 CXCR3-independent actions of CXCL10 may restrain cardiac fibrosis following myocardial infarction

CXCL10 null mice exhibited significantly accentuated fibrosis following myocardial infarction leading to worse remodelling;[9] in contrast, loss of CXCR3, the best-characterized CXCL10 receptor has no significant pro-fibrotic effects on the myocardium. Considering that, due to their low levels of expression in the infarcted heart, the other two CXCR3 ligands (CXCL9 and CXCL11) are unlikely modulators of the cardiac fibrotic response, how can we explain the distinct responses of CXCL10 and CXCR3 null animals following myocardial infarction?

Although a subpopulation of infarct myofibroblasts express CXCR3 (*Figure 1*), our experiments demonstrated that CXCL10-mediated modulation of fibroblast phenotype is independent of CXCR3 signalling. Inhibitory effects of CXCL10 on growth factor-induced cardiac fibroblast migration were observed in both WT and CXCR3 null cells (*Figure 6A*). Enzymatic disruption of HS and CS chains in cardiac fibroblasts abrogated the inhibitory effects of CXCL10 on cell migration, suggesting that proteoglycan signalling may mediate the anti-fibrotic actions of the chemokine. A growing body of evidence suggests an important role for proteoglycans in CXCL10-induced responses. Jiang *et al.*[13] demonstrated that CXCL10/syndecan-4 binding is implicated in mediating anti-fibrotic actions of CXCL10 in a model of pulmonary fibrosis. CXCR3-independent CXCL10 actions are not limited to fibroblasts; CXCL10 inhibition of endothelial cell proliferation correlated with glycosaminoglycan binding and not with CXCR3 signalling.[38]

4.4 Conclusions

Our findings suggest that the anti-fibrotic effects of CXCL10 in the infarcted heart are mediated through CXCR3-independent proteoglycan-mediated actions. These observations have important therapeutic implications in supporting therapeutic exploitation of the properties of CXCL10 in healing infarcts. Because CXCL10-induced CXCR3 signalling may activate T lymphocytes, inducing Th1-driven inflammation,[11,27] administration of CXCL10 protein defective in CXCR3 binding[13] may be effective in attenuating fibrotic remodelling of the infarcted ventricle, without stimulating potentially injurious inflammatory signalling.

Conflict of interest: none declared.

Funding

This work was supported by National Institutes of Health grants R01 HL76246 and R01 HL85440 (to N.G.F.), R01 AI39759 and R01 HL51365 (to C.G.).

References

1. Frangogiannis NG. Chemokines in ischemia and reperfusion. *Thromb Haemost* 2007;**97**:738–747.
2. Liehn EA, Postea O, Curaj A, Marx N. Repair after myocardial infarction, between fantasy and reality: the role of chemokines. *J Am Coll Cardiol* 2011;**58**:2357–2362.
3. Ivey CL, Williams FM, Collins PD, Jose PJ, Williams TJ. Neutrophil chemoattractants generated in two phases during reperfusion of ischemic myocardium in the rabbit. Evidence for a role for C5a and interleukin-8. *J Clin Invest* 1995;**95**:2720–2728.
4. Chandrasekar B, Smith JB, Freeman GL. Ischemia-reperfusion of rat myocardium activates nuclear factor-KappaB and induces neutrophil infiltration via lipopolysaccharide-induced CXC chemokine. *Circulation* 2001;**103**:2296–2302.
5. Dewald O, Zymek P, Winkelmann K, Koerting A, Ren G, Abou-Khamis T, Michael LH, Rollins BJ, Entman ML, Frangogiannis NG. CCL2/Monocyte Chemoattractant Protein-1 regulates inflammatory responses critical to healing myocardial infarcts. *Circ Res* 2005;**96**:881–889.
6. Nahrendorf M, Swirski FK, Aikawa E, Stangenberg L, Wurdinger T, Figueiredo JL, Libby P, Weissleder R, Pittet MJ. The healing myocardium sequentially mobilizes two monocyte subsets with divergent and complementary functions. *J Exp Med* 2007;**204**:3037–3047.
7. Dobaczewski M, Xia Y, Bujak M, Gonzalez-Quesada C, Frangogiannis NG. CCR5 signaling suppresses inflammation and reduces adverse remodeling of the infarcted heart, mediating recruitment of regulatory T cells. *Am J Pathol* 2010;**176**:2177–2187.
8. Frangogiannis NG, Mendoza LH, Lewallen M, Michael LH, Smith CW, Entman ML. Induction and suppression of interferon-inducible protein 10 in reperfused myocardial infarcts may regulate angiogenesis. *FASEB J* 2001;**15**:1428–1430.

9. Bujak M, Dobaczewski M, Gonzalez-Quesada C, Xia Y, Leucker T, Zymek P, Veeranna V, Tager AM, Luster AD, Frangogiannis NG. Induction of the CXC chemokine interferon-gamma-inducible protein 10 regulates the reparative response following myocardial infarction. *Circ Res* 2009;**105**:973–983.
10. Loetscher M, Gerber B, Loetscher P, Jones SA, Piali L, Clark-Lewis I, Baggiolini M, Moser B. Chemokine receptor specific for IP10 and mig: structure, function, and expression in activated T-lymphocytes. *J Exp Med* 1996;**184**:963–969.
11. Groom JR, Luster AD. CXCR3 in T cell function. *Exp Cell Res* 2011;**317**:620–631.
12. Soejima K, Rollins BJ. A functional IFN-gamma-inducible protein-10/CXCL10-specific receptor expressed by epithelial and endothelial cells that is neither CXCR3 nor glycosaminoglycan. *J Immunol* 2001;**167**:6576–6582.
13. Jiang D, Liang J, Campanella GS, Guo R, Yu S, Xie T, Liu N, Jung Y, Homer R, Meltzer EB, Li Y, Tager AM, Goetinck PF, Luster AD, Noble PW. Inhibition of pulmonary fibrosis in mice by CXCL10 requires glycosaminoglycan binding and syndecan-4. *J Clin Invest* 2010;**120**:2049–2057.
14. Hancock WW, Lu B, Gao W, Csizmadia V, Faia K, King JA, Smiley ST, Ling M, Gerard NP, Gerard C. Requirement of the chemokine receptor CXCR3 for acute allograft rejection. *J Exp Med* 2000;**192**:1515–1520.
15. Kroetz DN, Deepe GS Jr. An aberrant thymus in CCR5-/- mice is coupled with an enhanced adaptive immune response in fungal infection. *J Immunol* 2011;**186**:5949–5955.
16. Dewald O, Ren G, Duerr GD, Zoerlein M, Klemm C, Gersch C, Tincey S, Michael LH, Entman ML, Frangogiannis NG. Of mice and dogs: species-specific differences in the inflammatory response following myocardial infarction. *Am J Pathol* 2004;**164**:665–677.
17. Christia P, Bujak M, Gonzalez-Quesada C, Chen W, Dobaczewski M, Reddy A, Frangogiannis NG. Systematic characterization of myocardial inflammation, repair, and remodeling in a mouse model of reperfused myocardial infarction. *J Histochem Cytochem* 2013;**61**:555–570.
18. Bujak M, Ren G, Kweon HJ, Dobaczewski M, Reddy A, Taffet G, Wang XF, Frangogiannis NG. Essential Role of Smad3 in Infarct Healing and in the Pathogenesis of Cardiac Remodeling. *Circulation* 2007;**116**:2127–2138.
19. Chen W, Saxena A, Li N, Sun J, Gupta A, Lee DW, Tian Q, Dobaczewski M, Frangogiannis NG. Endogenous IRAK-M attenuates postinfarction remodeling through effects on macrophages and fibroblasts. *Arterioscler Thromb Vasc Biol* 2012;**32**:2598–2608.
20. Dobaczewski M, Bujak M, Li N, Gonzalez-Quesada C, Mendoza LH, Wang XF, Frangogiannis NG. Smad3 signaling critically regulates fibroblast phenotype and function in healing myocardial infarction. *Circ Res* 2010;**107**:418–428.
21. Saxena A, Chen W, Su Y, Rai V, Uche OU, Li N, Frangogiannis NG. IL-1 Induces proinflammatory leukocyte infiltration and regulates fibroblast phenotype in the infarcted myocardium. *J Immunol* 2013;**191**:4838–4848.
22. Engelhardt E, Toksoy A, Goebeler M, Debus S, Brocker EB, Gillitzer R. Chemokines IL-8, GROalpha, MCP-1, IP-10, and Mig are sequentially and differentially expressed during phase-specific infiltration of leukocyte subsets in human wound healing. *Am J Pathol* 1998;**153**:1849–1860.
23. Yates CC, Whaley D, Y-Chen A, Kulesekaran P, Hebda PA, Wells A. ELR-negative CXC chemokine CXCL11 (IP-9/I-TAC) facilitates dermal and epidermal maturation during wound repair. *Am J Pathol* 2008;**173**:643–652.
24. Flier J, Boorsma DM, van Beek PJ, Nieboer C, Stoof TJ, Willemze R, Tensen CP. Differential expression of CXCR3 targeting chemokines CXCL10, CXCL9, and CXCL11 in different types of skin inflammation. *J Pathol* 2001;**194**:398–405.
25. Flier J, Boorsma DM, Bruynzeel DP, Van Beek PJ, Stoof TJ, Scheper RJ, Willemze R, Tensen CP. The CXCR3 activating chemokines IP-10, Mig, and IP-9 are expressed in allergic but not in irritant patch test reactions. *J Invest Dermatol* 1999;**113**:574–578.
26. Panzer U, Steinmetz OM, Paust HJ, Meyer-Schwesinger C, Peters A, Turner JE, Zahner G, Heymann F, Kurts C, Hopfer H, Helmchen U, Haag F, Schneider A, Stahl RA. Chemokine receptor CXCR3 mediates T cell recruitment and tissue injury in nephrotoxic nephritis in mice. *J Am Soc Nephrol* 2007;**18**:2071–2084.
27. Groom JR, Luster AD. CXCR3 ligands: redundant, collaborative and antagonistic functions. *Immunol Cell Biol* 2011;**89**:207–215.
28. McInnis KA, Britain A, Lausch RN, Oakes JE. Synthesis of alpha-chemokines IP-10, I-TAC, and MIG are differentially regulated in human corneal keratocytes. *Invest Ophthalmol Vis Sci* 2005;**46**:1668–1674.
29. Frangogiannis NG, Lindsey ML, Michael LH, Youker KA, Bressler RB, Mendoza LH, Spengler RN, Smith CW, Entman ML. Resident cardiac mast cells degranulate and release preformed TNF-alpha, initiating the cytokine cascade in experimental canine myocardial ischemia/reperfusion. *Circulation* 1998;**98**:699–710.
30. Bujak M, Dobaczewski M, Chatila K, Mendoza LH, Li N, Reddy A, Frangogiannis NG. Interleukin-1 receptor type I signaling critically regulates infarct healing and cardiac remodeling. *Am J Pathol* 2008;**173**:57–67.
31. Laragione T, Brenner M, Sherry B, Gulko PS. CXCL10 and its receptor CXCR3 regulate synovial fibroblast invasion in rheumatoid arthritis. *Arthritis Rheum* 2011;**63**:3274–3283.
32. Yates CC, Whaley D, Kulasekeran P, Hancock WW, Lu B, Bodnar R, Newsome J, Hebda PA, Wells A. Delayed and deficient dermal maturation in mice lacking the CXCR3 ELR-negative CXC chemokine receptor. *Am J Pathol* 2007;**171**:484–495.
33. Yates CC, Krishna P, Whaley D, Bodnar R, Turner T, Wells A. Lack of CXC chemokine receptor 3 signaling leads to hypertrophic and hypercellular scarring. *Am J Pathol* 2010;**176**:1743–1755.
34. Jiang D, Liang J, Hodge J, Lu B, Zhu Z, Yu S, Fan J, Gao Y, Yin Z, Homer R, Gerard C, Noble PW. Regulation of pulmonary fibrosis by chemokine receptor CXCR3. *J Clin Invest* 2004;**114**:291–299.
35. Belperio JA, Keane MP, Burdick MD, Lynch JP 3rd, Xue YY, Li K, Ross DJ, Strieter RM. Critical role for CXCR3 chemokine biology in the pathogenesis of bronchiolitis obliterans syndrome. *J Immunol* 2002;**169**:1037–1049.
36. Wasmuth HE, Lammert F, Zaldivar MM, Weiskirchen R, Hellerbrand C, Scholten D, Berres ML, Zimmermann H, Streetz KL, Tacke F, Hillebrandt S, Schmitz P, Keppeler H, Berg T, Dahl E, Gassler N, Friedman SL, Trautwein C. Antifibrotic effects of CXCL9 and its receptor CXCR3 in livers of mice and humans. *Gastroenterology* 2009;**137**:309–319, 319 e301–303.
37. Burdick MD, Murray LA, Keane MP, Xue YY, Zisman DA, Belperio JA, Strieter RM. CXCL11 attenuates bleomycin-induced pulmonary fibrosis via inhibition of vascular remodeling. *Am J Respir Crit Care Med* 2005;**171**:261–268.
38. Campanella GS, Colvin RA, Luster AD. CXCL10 can inhibit endothelial cell proliferation independently of CXCR3. *PLoS One* 2010;**5**:e12700.